ELSEVIER

Journal of Crystal Growth 167 (1996) 260–264

JOURNAL OF CRYSTAL GROWTH

Growth rate models and kinetics estimation for $CaCO_3$ precipitated in continuous crystallizers

R. Isopescu, M. Mocioi, F. Zahanagiu, L. Filipescu *

University "Politehnica" of Bucharest, Polizu 1, 78168 Bucharest, Romania

Received 20 February 1995; accepted 8 May 1996

Abstract

Precipitation of $CaCO_3$ in a continuous crystallizer is analyzed on the basis of size-dependent growth rate models. The usefulness of such models is demonstrated by fitting them to several sets of experimental data consisting of the crystal size distribution measured under different operating conditions. The kinetic parameters, growth and nucleation rate thus estimated were correlated by empirical expressions in terms of *observables*. The growth rate of zero particle size has been found to increase with the augmentation of the desupersaturation rate and to decrease at higher suspension densities.

1. Introduction

The simulation, design and control of bulk suspension crystallizers are dependent on the accurate prediction of the crystal size distribution (CSD), which is determined by the kinetics and residence time distribution. The most common method for simultaneously determining nucleation and growth kinetics involves a mixed suspension mixed product removal (MSMPR) crystallizer operation and fitting then the experimental data to the appropriate growth models. In a large number of systems, non-linearity of the log population density versus size is observed over a wide range of crystal sizes. The main cause of such curvature seems to be the growth rate dispersion and/or size-dependent growth [1,2]. Several empirical equations for both mechanisms are recommended in the literature. In a recent work, Rojkowski [3] demonstrated that, at least from the mathematical point of view, there are two distinct phenomena that could produce the same type of CSD. It was demonstrated that the expression of mean growth rate for size L resulting from the growth dispersion may be combined with the population balance giving the equivalent form

$$\frac{\mathrm{d}}{\mathrm{d}L}\left[\bar{G}(L)n(L)\right] + \frac{1}{\tau}n(L) = 0. \qquad (1)$$

The mean rate $\bar{G}(L)$ may be replaced with the straight rate $G(L)$, thus, even if growth rate dispersion occurs, the experimental $n(L)$ data can be correlated with computed $\hat{n}(L)$ obtained by solving Eq. (1).

This paper attempts to present an analysis of CSD for $CaCO_3$ precipitated from CaO solution and CO_2 in a MSMPR crystallizer. The strong upward curvature of the experimental $\ln[n(L)]$ versus L was mainly assigned to size-dependent growth.

* Corresponding author.

PII S0022-0248(96)00088-7

2. Growth rate models

The population balance (1) was solved for some size-dependent growth rate models. The first is the well-known ASL equation proposed by Abegg et al. [4]

$$G(L) = G_0(1 + \gamma L)^b, \quad 0 \le b \le 1. \tag{2}$$

In this case, Eq. (1) has an analytical solution,

$$n(L) = n_0(1 + \gamma L)^{-b} \exp\left[\frac{1 - (1 + \gamma L)^{1-b}}{\gamma G_0 \tau (1 - b)}\right]. \tag{3}$$

The weakness of this model is the prediction of an infinite growth rate for $L \to \infty$. Some other models were proposed in the literature in order to overcome this inconvenience and to obtain finite values for the growth rate of large particles. We have chosen the three parameters exponential model [5] and a three parameter hyperbolic model [6]. The exponential model is given by the relation

$$G(L) = G_m - (G_m - G_0)\exp(-rL), \tag{4}$$

and the corresponding analytical solution of the population balance equation

$$n(L) = n_0 \exp\left(\frac{-L}{G_m \tau}\right)\left[\frac{G_0}{G(L)}\right]^{-1 + 1/rG_m\tau}. \tag{5}$$

The hyperbolic model is expressed by the relations

$$G(L) = \frac{G_0 + sG_m L}{1 + sL}, \tag{6}$$

$$n(L) = n_0 \exp\left(\frac{-L}{G_m \tau}\right)\left(\frac{G_0}{G(L)}\right)^{1+h}(1 + sh)^{-h}, \tag{7}$$

where

$$h = (G_m - G_0)/(sG_m^2\tau). \tag{8}$$

In these two models G_m represents the limiting growth rate for large crystal sizes, while r and s have no physical significance.

3. Experimental procedure

The experimental data concern the crystallization of $CaCO_3$ in a 1 litre MSMPR crystallizer, fed with CO_2 and CaO dissolved into a clear sucrose solution at steady state and pH values of 6.0–6.5. Fourteen runs have been carried out at 30°C, the suspension density varying between 1.96 and 35.71 kg/m^3, and the mean residence time ranging in the 640–4560 s interval.

The CSD was measured for crystals sampled out, after the crystallization process reached the steady state, using a laser beam particle sizer. The cumulative mass distribution has been converted into non-cumulative population density distribution.

4. Kinetic estimation

The parameter estimation is regarded as an optimization problem. The objective function commonly used is the least squares because this does not require any consideration of the experimental data structure. To our problem, this function is

$$F = \sum_{i=1}^{m} \left\{\ln[n(L_i)] - \ln[\hat{n}(L_i)]\right\}^2, \tag{9}$$

where $n(L_i)$ is the experimental population density according to Randolph and Larson's model, and $\hat{n}(L_i)$ is the population density computed from Eqs. (3), (5) and (7).

Luus and Jaakola's random adaptive search method [7] was used for the minimization of the objective function with respect to growth rate model parameters. As the correlation is carried out in terms of population density, n_0 must be also computed. If n_0 is regarded as the fourth searching variable, in spite of the high capability of Luus–Jaakola's algorithm to reach the global minima of a multimodal function, the surface generated by the objective function becomes inadequate for finding unambiguous values of the kinetics parameters. In this case, unreliable values for n_0 and G_0 could be reached. Extrapolating the best $\ln[\hat{n}(L)]$ outside the range of measured data, the surface generated by objective function is highly distorted, and the results lose their physical support. This fact has been observed also by Rojkowski [3], when dealing with the aluminium ammonium alum crystallization data. Midlarz and Jones [8], used a two parameter exponential growth rate model in order to avoid these difficulties. Their

model does not include parameters referring to zero crystal size. In the present paper this kind of model was not used. This model does not allow the estimation of the nucleation rate, because the extrapolation problem is not solved. We choose for n_0 estimation a simple parabolic extrapolation of the first three experimental data (which go down to 1 μm particle size) and the minimizing of the objective function (9) has been used for the identification of growth rate model parameters. The goodness of fit is given by the minimum value of the objective function, F_{min}, and this is the criterion of selection for the growth rate models.

5. Results

5.1. Parameter identification

The optimization problem defined by relation (9) was solved for fourteen experimental runs. The results obtained for the precipitation of $CaCO_3$ at 30°C and CaO 10 g/l in the feed stream are presented in Table 1. It can be noticed that the experimental CSD is better fit by the exponential model, though for small mean residence times all the three models give almost the same F_{min} value. The experimental data $n(L_i)$ collected from one run are plotted in Fig. 1 together with the correlation curves given by the ASL and the exponential model, respectively. In Fig. 2, the computed values of size-dependent growth rates are plotted against crystal size. The experimental growth rates are the values given by the experi-

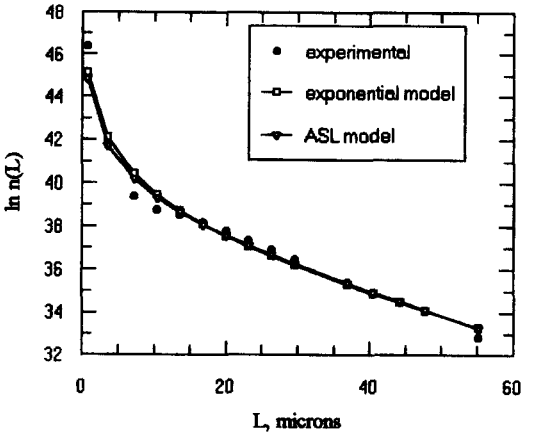

Fig. 1. Population density for precipitation at 30°C, 10 g/l CaO in the feed, mean residence time 4200 s.

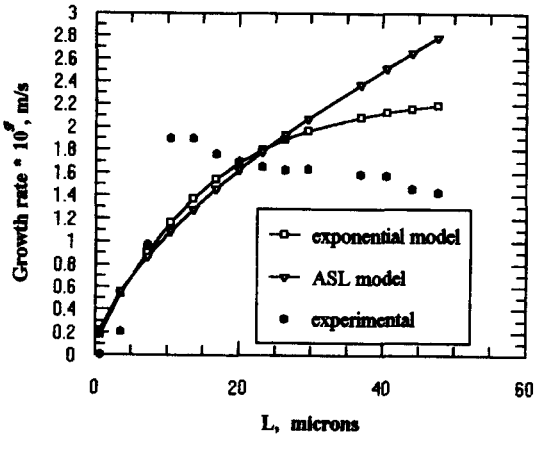

Fig. 2. Growth rates for precipitation at 30°C, 10 g/l CaO in the feed, mean residence time 4200 s.

Table 1
Kinetic parameters estimated for $CaCO_3$ precipitated at 30°C, 10 g/l CaO in the feed

Model	Mean residence time (s)	F_{min}	G_0 (m s^{-1})	B_0 (m^{-3} s^{-1})	G_m (m s^{-1})	Other parameters
Exponential	450	2.057	0.100×10^{-8}	6.423×10^{11}	0.195×10^{-7}	$r = 0.535 \times 10^5$
	1296	2.107	0.254×10^{-9}	2.695×10^{10}	0.558×10^{-8}	$r = 0.261 \times 10^5$
	4356	5.412	0.876×10^{-10}	2.540×10^{10}	0.229×10^{-8}	$r = 0.641 \times 10^5$
Hyperbolic	450	2.413	0.982×10^{-9}	6.308×10^{11}	0.321×10^{-7}	$s = 0.328 \times 10^5$
	1296	1.985	0.220×10^{-9}	2.340×10^{10}	0.622×10^{-8}	$s = 0.2835 \times 10^5$
	4356	6.043	0.968×10^{-10}	2.814×10^{10}	0.531×10^{-8}	$s = 0.2389 \times 10^5$
ASL	450	3.053	0.185×10^{-8}	1.182×10^{12}	–	$\gamma = 0.128 \times 10^7$, $b = 0.584$
	1296	4.910	0.355×10^{-9}	3.763×10^{10}	–	$\gamma = 0.226 \times 10^7$, $b = 0.472$
	4356	8.965	0.100×10^{-9}	3.002×10^{10}	–	$\gamma = 0.104 \times 10^8$, $b = 0.494$

mental CSD, using the White–Bending–Larson estimation method [9],

$$G(\bar{L}_i) = -\frac{1}{\tau}\frac{L_{i-1} - L_i}{\ln(N_{i-1}/N_i)}. \quad (10)$$

As can be noticed from Figs. 1 and 2, in the range of experimentally measured crystal sizes, the exponential model provides better approximation for the crystal growth rates and population density function.

The values of zero size crystal growth rates, G_0, estimated by the three models (see Table 1), have very close values. The limiting growth rates, G_m, are scattered, because of the ambiguity in G_m and r (or s) estimation and also due to the errors in the conversion of the cumulative into non-cumulative population density. The nucleation rate has been computed from the relation

$$B_0 = n_0 G_0. \quad (11)$$

5.2. Kinetic correlation

All the results may be correlated by empirical power-law kinetic expressions in terms of *observables*. Such equations have been developed for G_0, G_m and B_0 as a function of suspension density, m_t and the rate of *desupersaturation* defined as

$$\frac{\delta c}{\tau} = \frac{Q_i c_i - Q_e c}{Q_i \tau}. \quad (12)$$

We assume that this rate depends on the supersaturation in a MSMPR crystallizer.

The correlation parameters were estimated by a least-squares multiple linear regression analysis. The fit of the equations is reflected by the correlation coefficient, R^2. The 95% confidence limits of the power exponents were found using Student's t-test.

The correlation equations for G_0, G_m, B_0 data are based on the values of the exponential growth rate model, which had the greatest ability to fit the CSD data.

$$G_0 = 1.250 \times 10^{-6}\left(\frac{\delta c}{\tau}\right)^{1.001 \pm 0.058}(m_t)^{-1.310 \pm 0.051},$$

$$R^2 = 0.977, \quad (13)$$

$$G_m = 7.218 \times 10^{-6}\left(\frac{\delta c}{\tau}\right)^{0.995 \pm 0.133}(m_t)^{-0.886 \pm 0.118},$$

$$R^2 = 0.873, \quad (14)$$

$$B_0 = 2.669 \times 10^{13}\left(\frac{\delta c}{\tau}\right)^{1.1622 \pm 0.320}(m_t)^{-0.234 \pm 0.281},$$

$$R^2 = 0.751. \quad (15)$$

6. Discussions and conclusions

The analysis of $CaCO_3$ precipitation in terms of the growth rate models showed that the shape of CSD can be explained by the size-dependent growth rate. The exponential and hyperbolic models gave almost the same goodness of fit and they accounted for the experimental CSD in almost all runs. The hyperbolic model can generally reflect a steep slope of $\ln[n(L)]$ function in the small ranges of the crystal sizes. According to our way of n_0 estimation, very steep slopes beyond the experimental points are not to be expected.

At long mean residence times and high suspension densities, the size-dependent growth rate models have a poor fit to the experimental CSD. In these experiments an unexpected drop of the population density in the neighbourhood of small particle sizes is revealed. This may be due to other phenomena such as breakage of the particles as the phase transition amorphous–calcite proceeds [10]. These runs have been overlooked in the kinetic correlation procedure.

The power exponents in the kinetic correlation show a linear proportionality between the growth rate and the desupersaturation rate. The large crystal growth rates are evenly controlled by the desupersaturation rate, as diffusion control has no significance. The growth rates decrease with increasing magma density, m_t. The nucleation rate, B_0 is relatively independent of suspension density. The explanation may lie in the high speed of the chemical reaction generating nuclei. Also, the discontinuity in n_0 and G_0 estimation may account for this occurrence, as well as for the poor correlation coefficient R^2.

The analysis of $CaCO_3$ precipitation on the basis of size-dependent growth rate models and kinetics

correlation gives some insight of the process and offers some explanations of the distorted shape of the experimental CSD.

List of symbols

b Parameter in ASL model
B_0 Nucleation rate (m^{-3} s^{-1})
c_i Concentration in the inlet flow rate (kg m^{-3})
G Growth rate (m s^{-1})
G_0 Growth rate for zero size (m s^{-1})
G_m Maximum growth rate (m s^{-1})
L Crystal size (m)
$\bar{L}$ Arithmetic average of crystal size (m)
m_t Suspension density (kg/m^3)
n, $\hat{n}$ Population density (m^{-4})
n_0 Nuclei density (m^{-4})
N Cumulative oversize distribution (m^{-3})
r Parameter in exponential model
s Parameter in hyperbolic model
Q_i Inlet flow rate (m^3 s^{-1})
Q_e Outlet flow rate (m^3 s^{-1})
δ Difference
γ Parameter in ASL model
τ Mean residence time (s)

References

[1] J. Garside, V.R. Philips and M.B. Shah, Ind. Chem. Fund. 15 (1976) 230.
[2] A.H. Janse and E.J. de Jong, Industrial Crystallization (Plenum, New York, 1976) p. 145.
[3] Z. Rojkowski, Chem. Eng. Sci. 48 (1993) 1475.
[4] C.F. Abegg, J.D. Stevans and M.A. Larson, AIChE J. 14 (1968) 118.
[5] Z. Rojkowski, Krist. Technik 12 (1977) 1121.
[6] Z. Rojkowdki, Bull. Acad. Polon. Sci. Ser. Sci. Chim. 26 (1978) 265.
[7] R. Luus and T.H. Jaakola, AIChE J. 18 (1973) 760.
[8] J. Midlarsz and A.G. Jones, Comp. Chem. Eng. 13 (1989) 959.
[9] E.T. White, L.L. Bendig and M.A. Larson, AIChE J. Symp. Ser. 72 (1976) 41.
[10] L. Filipescu, M. Mocioi, A. Zaharia and M. Cretu, Rev. Chim. 32 (1981) 347.